Evidence for the role of ion-induced particle formation during an atmospheric nucleation event observed in Tropospheric Ozone Production about the Spring Equinox (TOPSE)

Vijay Kanawade and S. N. Tripathi

Department of Civil Engineering, Indian Institute of Technology, Kanpur, India

Received 14 June 2005; revised 14 October 2005; accepted 20 November 2005; published 31 January 2006.

[1] Various in situ measurements show evidence of new particle formation over a wide range of latitudes in the middle to upper troposphere and lower stratosphere. However, the exact mechanism of new particle formation is still uncertain. Using a combination of satellite-derived brightness temperature, air parcel backward trajectory information, in situ measurements of aerosol and precursor gases and an aerosol microphysical model driven by parameterized ion-induced nucleation, we investigate the mechanism responsible for, and factors leading to, new particle formation in the middle to upper troposphere during the Tropospheric Ozone Production about the Spring Equinox (TOPSE) experiment. The number concentrations of modeled ultrafine particles of diameters 3 to 4 nm (N_{3-4nm}) and 3 to 8 nm (N_{3-8nm}) are consistent with in situ measurements indicating that new particle formation likely occurred by ion-induced nucleation a day prior to the time of measurement. A reduction in preexisting aerosol surface area in a region of cloud outflow probably triggered particle nucleation. These studies indicate that under typical middle to upper troposphere conditions, the ion mechanism is likely an important source of ultrafine particles, and these newly formed particles can grow to act as cloud condensation nuclei.

Citation: Kanawade, V., and S. N. Tripathi (2006), Evidence for the role of ion-induced particle formation during an atmospheric nucleation event observed in Tropospheric Ozone Production about the Spring Equinox (TOPSE), *J. Geophys. Res.*, *111*, D02209, doi:10.1029/2005JD006366.

1. Introduction

[2] Ultrafine particles are ubiquitous in the Earth's atmosphere and have received increasing attention because of their possible impacts on global climate and health [*Kulmala*, 2003]. The upper troposphere and lower stratosphere (UTLS) region is a source of new particles [*Brock et al.*, 1995; *Schröder and Ström*, 1997; *De Reus et al.*, 1999; *Nyeki et al.*, 1999; *Wang et al.*, 2000; *Hermann et al.*, 2003; *Lee et al.*, 2003]. Species participating in particle formation include sulfuric acid and water, plausibly ammonia, and possibly some organic vapors [*Coffman and Hegg*, 1995; *Marti et al.*, 1997]. New particles are formed under the typical UTLS conditions of SO_2 concentrations, temperature, and relative humidity, with sufficient sun exposure and low preexisting aerosol surface area [*Lee et al.*, 2003]. These newly formed particles may grow to cloud condensation nuclei, which play an important role in cloud formation and hence have an impact on global and regional climate [*Lee et al.*, 2004].

[3] Several different nucleation mechanisms have been proposed to explain atmospheric particle formation, including binary homogeneous nucleation (BHN) of sulfuric acid–water (H_2SO_4-H_2O) [*Seinfeld and Pandis*, 1998; *Vehkamäki et al.*, 2002], ternary homogeneous nucleation (THN) of sulfuric acid-ammonia-water (H_2SO_4-NH_3-H_2O) [*Kulmala et al.*, 2000; *O'Dowd et al.*, 2002], and ion-induced nucleation (IIN) [*Yu and Turco*, 2001; *Laakso et al.*, 2002; *Lee et al.*, 2003; *Lovejoy et al.*, 2004]. However, at present, it is unclear which nucleation mechanism dominates in the atmosphere [*Kulmala*, 2003]. The BHN and THN have been widely used to explain new particle formation. However, there are large uncertainties in the predictions of classical homogenous nucleation theory due to the use of macroscale thermodynamic concepts such as surface tension that are required by the model. Most models of BHN and THN, in their current state, have not been evaluated for free tropospheric conditions [*Lee et al.*, 2003]. IIN has been suggested to explain the new particle formation observed in the UTLS region [*Lee et al.*, 2003; *Lovejoy et al.*, 2004]. The high relative humidity in the vicinity of clouds makes this region a favorable environment for new particle formation. Evidence for new particle formation near marine cumulus clouds has been found earlier [*Hegg et al.*, 1991; *Perry and Hobbs*, 1994; *Clarke et al.*, 1998, *Weber et al.*, 2001]. The outflow of large convective clouds has also been suggested to be an area of in situ new particle formation [*Wang et al.*, 2000; *Clarke et al.*, 1999].

[4] In this paper, we use an efficient and fast aerosol microphysical model with ion-induced nucleation to interpret in situ measured new particle formation in the middle to

0148-0227/06/2005JD006366$09.00

upper troposphere. Using a combination of backward air parcel trajectory analysis, brightness temperature retrieved from satellite cloud images, in situ aerosol and precursor gaseous measurements, and microphysical modeling, we investigate the role of environmental factors leading to new particle formation in the middle to upper troposphere during an atmospheric nucleation event measured. These studies serve to test the ability of the microphysical model to reproduce the in situ measured particle number concentrations during atmospheric nucleation events in the middle to upper troposphere region. A brief model overview is given in the next section.

2. Model Overview

[5] *Tripathi et al.* [2004] (available at http://www.atm.ox.ac.uk/main/research/technical.html) developed a fast H_2SO_4-H_2O aerosol microphysical model (SAMM) that simulates homogeneous binary nucleation, H_2SO_4 condensational growth and evaporation, water vapor equilibrium, particle-particle coagulation and sedimentation removal. These aerosol processes are solved using a noniterative semi-implicit scheme with integration time step of 60 s [*Jacobson*, 2002]. The model covers particle sizes from 0.3 nm to 3 μm diameter, which are geometrically divided into 40 bins. The model has been evaluated against observed data for background stratospheric aerosol size distribution [*Tripathi et al.*, 2004].

[6] In the H_2SO_4-H_2O aerosol microphysical model, new particle formation, which was earlier treated as homogeneous binary nucleation, is replaced by an ion-induced nucleation (IIN) parameterization. This model will hereafter be referred to as SAMIN model. The IIN parameterization was developed by *Modgil et al.* [2005] using laboratory measured thermodynamic data for the growth and evaporation of small cluster ions containing sulfuric acid and water, to yield quantitative predictions of the rate of ion-induced nucleation for atmospheric conditions [*Lovejoy et al.*, 2004]. This IIN parameterization is valid for a wide range of environmental parameters, e.g., 200 $\leq$ temperature (T) $\leq$ 280 K, 0.05 $\leq$ relative humidity (RH) $\leq$ 0.95, $10^5 \leq$ sulfuric acid gas concentration (H_2SO_4) $\leq 10^8$ molecules cm^{-3}, 2 $\leq$ surface area of preexisting aerosol (SA) $\leq$ 100 μm^2 cm^{-3}, 2 $\leq$ ion production rate (Q) $\leq$ 30 ion pairs cm^{-3} s^{-1}. This range of environmental parameters covers the variation found in the UTLS region globally. The parameterized nucleation rate generally reproduces the explicitly modeled ion-assisted nucleation rate within an order of magnitude over the whole range of conditions, except when the nucleation rate is very low ($<10^{-6}$ cm^{-3} s^{-1}), which corresponds to a rate of less than 0.1 particle day^{-1} cm^{-3} [*Modgil et al.*, 2005]. *Lovejoy et al.* [2004] have described the theory and procedure used to calculate particle nucleation rate.

[7] The parameterized particle nucleating flux in SAMIN is calculated as a function of T, RH, number of sulfuric acid molecules in the average nucleating cluster, Q, and SA. The total aerosol surface area (SA_t) integrated over aerosol particles of all sizes is calculated as

$$SA_t = \sum_{i=1}^{40} \pi d_i^2 N_{i,t} \quad (1)$$

where d_i is the diameter of particle and $N_{i,t}$ is the number concentration of particles in a size bin i at time t. The total surface area in the SAMIN model is updated at every time step with the equation (1). In the model, sulfuric acid production is calculated from the atmospheric precursor gases SO_2 and OH. In the upper troposphere, the rate-limiting reaction for the production of gas phase H_2SO_4 is the reaction of OH with SO_2:

$$\left(\frac{\partial H_2SO_4}{\partial t}\right) = f(K_0, K_\infty)[OH][SO_2] \quad (2)$$

where $F(K_0, K_\infty)$ denotes the rate constants for the association reaction [OH + SO_2 → H_2SO_4] and depends on ambient temperature and pressure, ranging from 7 to 9 × 10^{-13} cm^{-3} s^{-1} [*DeMore et al.*, 1997].

$$f(K_0, K_\infty) = \left(\frac{K_0[M]}{1 + K_0[M]/K}\right) 0.6^{\left(1+\left(\log\frac{K_0[M]}{K}\right)\right)}$$

$K_0 = 3.0 \times 10^{-31} \times (T/300)^{-3.3}$ cm^6 molecule^{-2} s^{-1} and $K_\infty = 1.5 \times 10^{-12}$ cm^3 molecule^{-1} s^{-1}. [M] = [N_2] + [O_2] is the number concentration (molecules cm^{-3}) of the third body.

[8] Since particle nucleation and H_2SO_4 condensational growth are coupled in the SAMIN model, the nucleation rate is first converted to a mass transfer rate between H_2SO_4 gas and particle, and is then added to the particle mass growth rate in the size bin i. The particle mass growth rate ($k_{i,t-\Delta t}$) can be approximated as

$$k_{i,t-\Delta t} = 2\pi N_{i,t-\Delta t} d_i D_i^{eff} \quad (3)$$

where D_i^{eff} is the effective diffusion coefficient of H_2SO_4 (cm^2 s^{-1}) [*Jacobson and Turco*, 1995] and $N_{i-\Delta t}$ is the number concentration of particles in size bin i at previous time $t - \Delta t$. The corresponding gas phase mass transfer rate can be written as *Jacobson* [2002],

$$k_{i,t-\Delta t}^{nuc} = h_1 \frac{\pi \rho_{H2SO4} h_5^3 f_i}{6 m_{H2SO4}} \left(\frac{1}{C_{t-\Delta t} - S_{i,t-\Delta t} C_{i,t-\Delta t}^{sat}}\right) \quad (4)$$

where h_1 is the parameterized particle nucleating flux (cm^{-3} s^{-1}), h_5 is the parameterized diameter of critical cluster (cm), ρ_{H2SO4} is the density of pure sulfuric acid (g m^{-3}), f_i is the volume fraction of sulfuric acid in critical cluster, m_{H2SO4} is the molecular weight of sulfuric acid (g mole^{-1}), $C_{t-\Delta t}$ is the H_2SO_4 concentration (mole cm^{-3}), $S_{i,t-\Delta t}$ is saturation ratio of H_2SO_4 above a curved surface of pure sulfuric acid, $C_{i,t-\Delta t}^{sat}$ is the saturation vapor mole concentration of condensing H_2SO_4 above a flat surface having the same composition as the droplet in bin i. The gas phase transfer rate calculated from equation (4) is then added to the particle mass growth rate, calculated from equation (3), for the bin size where all the nucleated particles are placed.

[9] Once new particles are formed and if the vapor pressure of H_2SO_4 is in excess of the equilibrium vapor pressure, these newly formed particles undergo sulfuric acid condensation as described by *Jacobson* [1997, 1999]. As particles grow, they are brought to thermodynamic equilib-

rium with respect to ambient water vapor pressure. Condensation and coagulation are coupled in an operator-split manner. Number concentrations determined from the condensation solution are used to initialize values before coagulation. Further details of the model are given by *Tripathi et al.* [2004].

3. Comparison Between Parameterized and Explicit Ion-Induced Nucleation Models

[10] In this section, it will be shown that the parameterized SAMIN model predicts number concentrations of particles of diameter greater than 3 nm ($N_{>3nm}$) and particle size distributions that closely follow those predicted by the explicit Sulfuric Acid and Water Nucleation (SAWNUC) model of ion-assisted nucleation [*Lovejoy et al.*, 2004]. The purpose is to demonstrate the capability of the SAMIN model in reproducing the SAWNUC model predictions of $N_{>3nm}$ and particle size distributions, for the environmental conditions in the UTLS region. The SAWNUC model explicitly treats the ions and electrical charges on particle and their effects on condensation and coagulation processes, and thus it is computationally slower than SAMIN by an order of magnitude. With geometrically spaced size bins (around 40 bins for particles in the range 0.3 nm to 3 μm) and a 60 s time step, SAMIN takes ~0.42 s of CPU time on Pentium IV, 1.0 GHz computer to calculate a particle size distribution, whereas SAWNUC takes ~4.0 s. The CPU time taken by the computer code is a concern when one wants to perform large number of calculations and/or if the code is intended for implementation in a global model. As shown below, the SAMIN model, which does not take into account the effect of charge on microphysical processes, and which uses a parameterized IIN particle flux (h_1, cm^{-3} s^{-1}) and diameter of average nucleating cluster (h_5, cm), is able to reproduce the SAWNUC predictions of particle size distribution and $N_{>3nm}$ with reasonable agreement.

[11] Both the models were run for environmental conditions typical for particle nucleation in the middle to upper tropospheric region. Both models were run for 12 hours of daylight. For these simulations, the base conditions are chosen as follows: (1) H_2SO_4 concentrations were assumed to be constant for the 12-hour run, (2) the initial particle size distribution in SAMIN was prescribed to be exactly same as that of SAWNUC at time $t = 0$, and (3) the initial preexisting aerosol surface area was assumed to be 5 μm^2 cm^{-3} and was updated at every time step with the equation (1). Figure 1 shows a comparison between SAWNUC and SAMIN calculations of $N_{>3nm}$ for a range of T (195–280 K), RH (0.05–0.95), H_2SO_4 (10^6–10^8 molecules cm^{-3}), Q (2–30 ion pairs cm^{-3} s^{-1}) and SA (2–50 μm^2 cm^{-3}).

[12] From Figures 1a–1f, it can be seen that the SAMIN model simulation of $N_{>3nm}$ are generally within a factor of 4 with those from the SAWNUC model. In Figure 1a, $N_{>3nm}$ suddenly decrease for $T > 260$ K and the SAWNUC and SAMIN models do not agree well. However, since $T > 260$ K represents the lower troposphere, it is of little significance for the present study. It can be seen from Figure 1c that as RH increases, $N_{>3nm}$ increases up to RH = 0.25 and 0.2 for $Q = 2$ and 30, respectively, and then becomes constant with increasing RH. From Figure 1d, it is evident that as sulfuric acid concentration increases, $N_{>3nm}$ decreases because of condensational growth on already nucleated particles dominating over particle nucleation. It is also clear that $N_{>3nm}$ calculated by both models are in excellent agreement for $T = 220$ and 250 K. Figure 1e depicts the variation of $N_{>3nm}$ as a function of ion production rates for RH = 0.2 and 0.4 and $N_{>3nm}$ predicted by SAMIN is within a factor of 2 of that predicted by SAWNUC. Figure 1f shows that particle production by ion-induced nucleation decreases as surface area increases, a trend well captured by SAMIN.

[13] While $N_{>3nm}$ is a useful parameter for evaluating particle nucleation rates, in a variety of situations, for example, in assessing the role of these particles as potential cloud condensation nuclei, the exact nature of particle size distribution becomes important. We have compared SAMIN and SAWNUC predictions of particle size distribution for the environmental conditions (1) $220 \leq T \leq 265$ K, (2) RH = 0.6, (3) $10^5 \leq H_2SO_4 \leq 10^8$ molecules cm^{-3}, (4) SA (at time t = 0) = 5 μm^2 cm^{-3}, and (5) $10 \leq Q \leq 30$ ion pairs cm^{-3} s^{-1} (Figure 2). The particle size distributions calculated by the SAMIN model were compared with the SAWNUC model to evaluate whether the salient characteristics, such as presence of single mode diameter, are consistent with those predicted by SAWNUC model. Figures 2a and 2b give particle size distribution comparisons for environmental conditions representative of the middle to upper troposphere region. These size distributions are usually unimodal, with peaks at diameter ~ 1–2, 9–12 and 80–100 nm for $H_2SO_4 = 10^6$, 10^7 and 10^8 molecules cm^{-3} respectively after the 12-hour model simulation. Figure 2d gives particle size distribution comparison for different ion production rates. In general, the difference between particle size distribution parameters calculated from SAMIN and SAWNUC models compare well relative to the large disagreements between model and observation reported, for example, by *Uhrner et al.* [2003].

4. New Particle Formation in the Free Troposphere

[14] In this section we analyze, in detail, the ultrafine particle number concentrations of diameters 3–4 and 3–8 nm (N_{3-4nm} and N_{3-8nm}) observed during the TOPSE nucleation event. *Weber et al.* [1999] summarized simultaneous in situ measurements of the likely nucleation precursor species (i.e., OH, and SO_2), ultrafine particles, T, RH, etc., in the remote troposphere atmospheric nucleation events. Such simultaneous in situ measurements of atmospheric parameters permit comparison between model-predicted ultrafine particle concentrations and observed data.

[15] The TOPSE experiment was conducted during February–May 2000 to study the evolution of tropospheric chemistry at middle to high latitudes (50°–90°W longitude and 60°–85°N latitude) from 100 to 25,000 feet in altitude, over North America. The experiment used airborne in situ and remote sensing measurements of trace gases, radiation, and aerosols, combined with model simulations. This was an exploratory mission to investigate, in part, if photochemical production of vapors, like sulfuric acid, could be significant in situ source of new particles. *Weber et al.* [2003] summarized that new particle production tended to be found in plumes that contained high concentrations of sulfur dioxide and sulfuric acid; however it was unclear

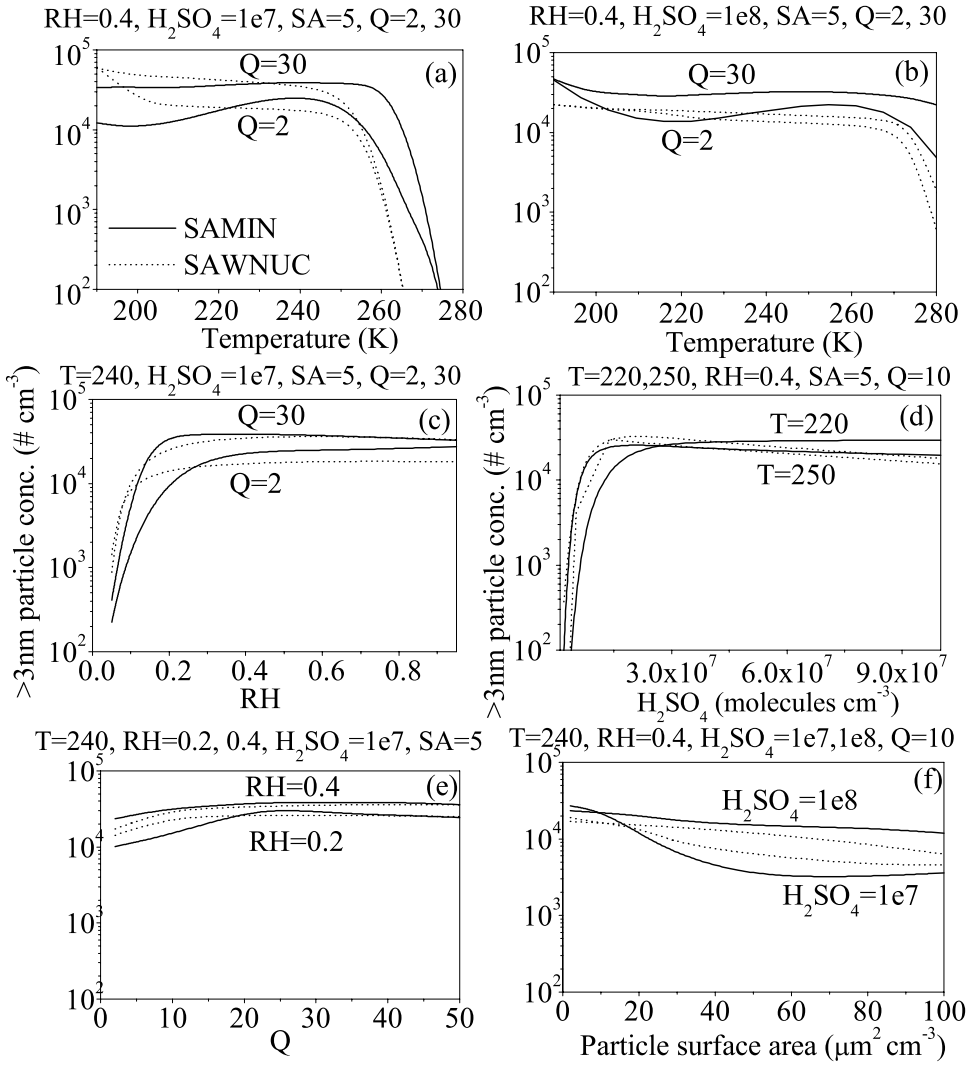

Figure 1. Comparison between SAMIN and SAWNUC predicted >3 nm particle number concentrations for environmental conditions: (a) RH = 0.40, $H_2SO_4 = 10^7$ molecules cm^{-3}, SA = 5 μm^2 cm^{-3}, and $Q = 2$ and 30 ion pairs cm^{-3} s^{-1}. (b) Same as Figure 1a except for $H_2SO_4 = 10^8$ molecules cm^{-3}. (c) $T = 240$ K, $H_2SO_4 = 10^7$ molecules cm^{-3}, SA = 5 μm^2 cm^{-3}, and $Q = 2$ and 30 ion pairs cm^{-3} s^{-1}. (d) $T = 220$ and 250 K, RH = 0.40, SA = 5 μm^2 cm^{-3}, and $Q = 10$ ion pairs cm^{-3} s^{-1}. (e) $T = 240$ K, RH = 0.2 and 0.4, $H_2SO_4 = 10^7$ molecules cm^{-3}, and SA = 5 μm^2 cm^{-3}. (f) $T = 240$ K, RH = 0.4, $H_2SO_4 = 10^7$ and 10^8 molecules cm^{-3}, and $Q = 10$ ion pairs cm^{-3} s^{-1}.

whether the observed particles with diameter >3 nm were produced in situ or transported from lower latitudes. Another question was whether the particles were produced on the same day of observation or whether the nucleation was occurred on previous days. The in situ measured parameters T, RH, H_2SO_4, SO_2, OH, N_{3-4nm} and N_{3-8nm} for TOPSE experiment are available at http://topse.acd.ucar.edu/data/, and a complete overview of the TOPSE study is given by *Atlas et al.* [2003].

[16] A unique region of high N_{3-4nm} associated with concentrations of SO_2 of 3.5 ppbv was detected on 7 March 2000. On this day the highest concentration of SO_2 and sulfuric acid were observed at altitudes from ~3 to ~5 km. Although $N_{>3nm}$ were also high, N_{3-4nm} and N_{3-8nm} were observed only in a narrow altitude range from approximately 4.0 to 4.2 km (1600–1615 GMT) [*Weber et al.*, 2003]. The presence of these ultrafine particles is an indication for recent particle production since these particles are so small that they have to be produced in situ in the atmosphere [*De Reus et al.*, 1999].

[17] Because observed RH was too low to allow particle nucleation in the region of ultrafine particle enhancements observed in TOPSE, it is believed that rain event that scavenged aerosol particles, allowed sulfuric acid source strength to increase and preexisting aerosol surface area to decrease, could have triggered particle nucleation earlier in this parcel. Knowledge of backward air parcel trajectory and cloud top temperature retrieved from satellite cloud images can be used to directly relate the presence of ultrafine condensation nuclei to the occurrence of convection [*De Reus et al.*, 2001]. Therefore we have analyzed backward trajectory of air parcel and brightness temperature from

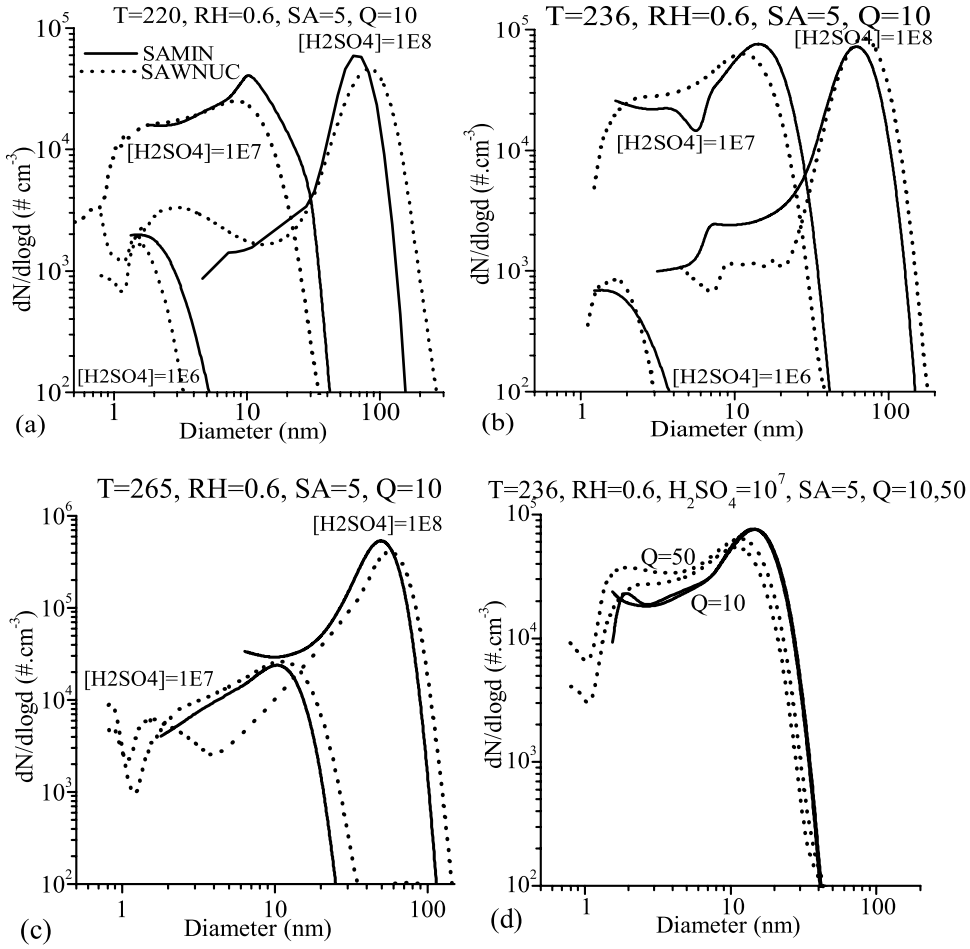

Figure 2. Comparison between SAMIN and SAWNUC model-calculated particle size distribution for environmental conditions: (a) $T = 220$ K, RH = 0.6, SA = 5 μm^2 cm^{-3}, $Q = 10$ ion pairs cm^{-3} s^{-1}, and $H_2SO_4 = 10^6$, 10^7, and 10^8 molecules cm^{-3}. (b) Same as Figure 2a except for $T = 236$ K. (c) $T = 265$ K, RH = 0.6, SA = 5 μm^2 cm^{-3}, $Q = 10$ ion pairs cm^{-3} s^{-1}, and $H_2SO_4 = 10^7$ and 10^8 molecules cm^{-3}. (d) $T = 236$ K, RH = 0.6, SA = 5 μm^2 cm^{-3}, $H_2SO_4 = 10^7$ molecules cm^{-3}, and $Q = 10$, 50 ion pairs cm^{-3} s^{-1}.

satellite cloud images to see whether the air parcel came in contact with clouds.

[18] The cloud top temperature is the atmospheric air temperature at the top of cloud, which can be computed using CO_2 absorption technique based on Planck's radiation equation. However, it requires that brightness temperature (and consequently radiance) measurements were made using 13.3 μm infrared band. To the best of our knowledge, GOES 10 is the only satellite that covers our region of study (western Canada). Since the GOES 10 imager (11.0 μm) does not have a 13.3 μm infrared band in that region for year 2000, we directly use brightness temperature as atmospheric air temperature at the top of the cloud with crude assumptions. There are several instances when the observed cloud 11.0 μm brightness temperature and the atmospheric air temperature at the top of the cloud (cloud top temperature) are equal (or nearly equal). The controlling factor is the thickness or the opacity of the cloud. If the thickness of cloud is 5 to 10 km or more (emissivity ≈ 1.0), the cloud top temperature (or the observed brightness temperature in the longwave window) and the atmospheric air temperature at the top of the cloud will be nearly equal. On the other hand, if the cloud is thin or transparent (emissivity < 0.3), the observed brightness temperature will be warmer than the atmospheric air temperature at the top of cloud. The temperature difference between the cloud top temperature and 11.0 μm brightness temperature is indirectly related to the thickness (emissivity) of the cloud. For thicker cloud (emissivity ≈1.0) the difference between the two measurements would be small (usually <1 K), while for thin clouds (emissivity < 0.3 and depending on the altitude of the thin clouds in the atmosphere) the difference can be 5–10 K [*Schreiner et al.*, 2001].

5. A Case Study of 7 March: Simulation of N_{3-4nm} and N_{3-8nm} Particles

[19] In this section, we evaluate whether the model-predicted N_{3-4nm} and N_{3-8nm} are consistent with the in situ measurements during the TOPSE experiment research flight of 7 March 2000 (size distribution were not measured). For each flight level, the difference in brightness temperature and the temperature along the air parcel back trajectory is used to determine if the air mass has

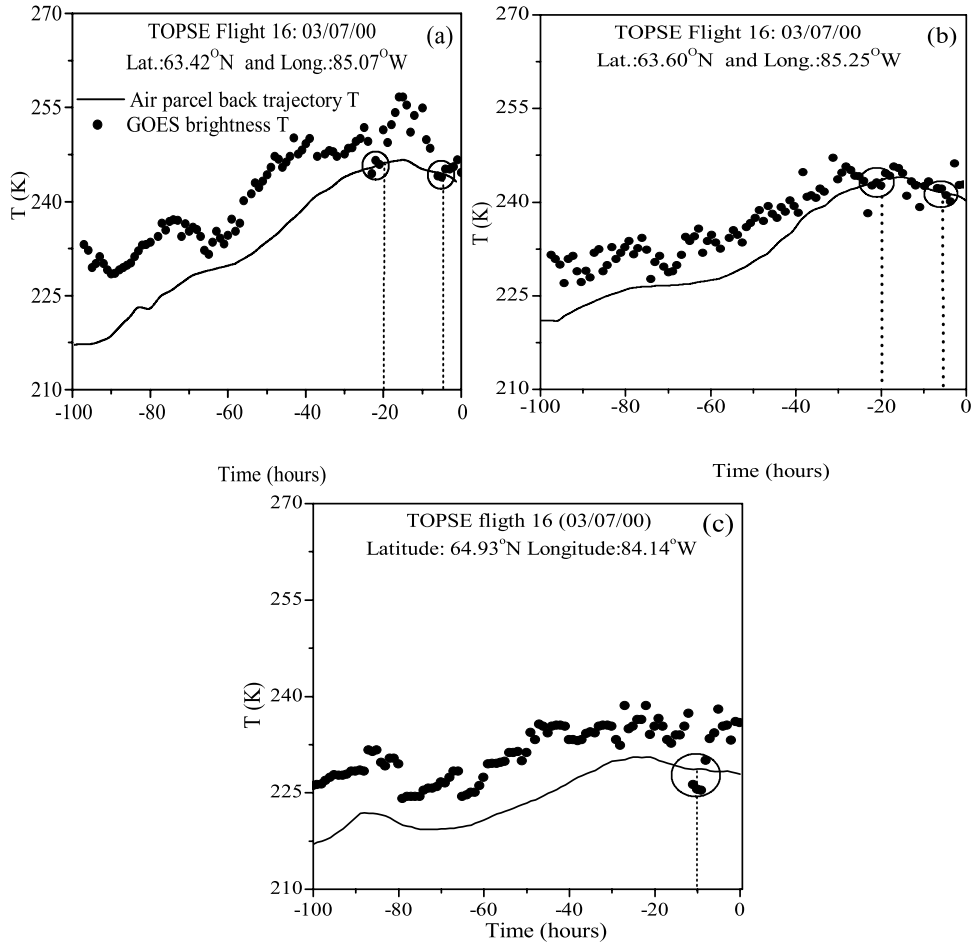

Figure 3. (a) Brightness temperature (solid circles) retrieved from GOES 10 satellite hourly cloud images and air parcel temperature (solid line) along 5-day backward trajectory calculated using NOAA Air Resources Laboratory HYSPLIT transport model, starting at latitude of 63.42°N and longitude of 85.07°W. (b) Same as Figure 3a except for latitude of 63.60°N and longitude of 85.25°W within nucleation region. (c) Same as Figure 3a except for latitude of 64.93°N and longitude of 84.14°W above nucleation region. Open circles show location where air parcel is likely to come into contact with the clouds.

been in contact with clouds during the last 5 days of its transport toward the measurement region. Five-day backward trajectory calculations were performed using the NOAA Air Resources Laboratory (ARL) Hybrid Single-Particle Lagrangian Integrated Trajectory (HYSPLIT) program (http://www.arl.noaa.gov/ready/hysplit4.html) using the final run data archive of the GDAS model for each flight level in the middle troposphere. Along the track of the backward trajectory the brightness temperature was retrieved, using the infrared channel of the GOES 10 satellite. Every hour the satellite image is updated, so that the brightness temperature of air mass passing over a certain location can be retrieved. Figure 3 shows comparisons between brightness temperature as retrieved from satellite cloud images and air parcel temperatures calculated using HYSPLIT program along a 5-day backward trajectory for three different starting points: latitude of 63.42°N and longitude of 85.07°W (Figure 3a), latitude of 63.60°N and longitude of 85.25°W within nucleation region (Figure 3b), and latitude of 63.60°N and longitude of 85.25°W above the nucleation region (Figure 3c). From Figure 3, it can be seen that the air parcel likely came into contact with clouds at −20 and −5 hours from the time of measurement for Figures 3a and 3b and at −10 hours for Figure 3c.

[20] Five-day multiple back trajectories calculated using the HYSPLIT model PC version (Figure 4) from the time of observation suggest that there was not much evidence for variation in air mass origin or for differential vertical advection between air masses during their transport toward the measurement region. The model was run from previous day until the time of measurement because over the high latitudes the particle growth rate can be as low as 0.1 nm h^{-1} [*Kulmala et al.*, 2004] and since newly formed particles have sizes ~1 nm that will take almost a day to grow to 3–8 nm sizes. The model was run using the parcel *T* and RH as calculated from the backward trajectory simulations, from the time when the air parcel was likely to come into contact with the clouds (−20 hours from measurement time). Nucleation in the model was disabled during night hours.

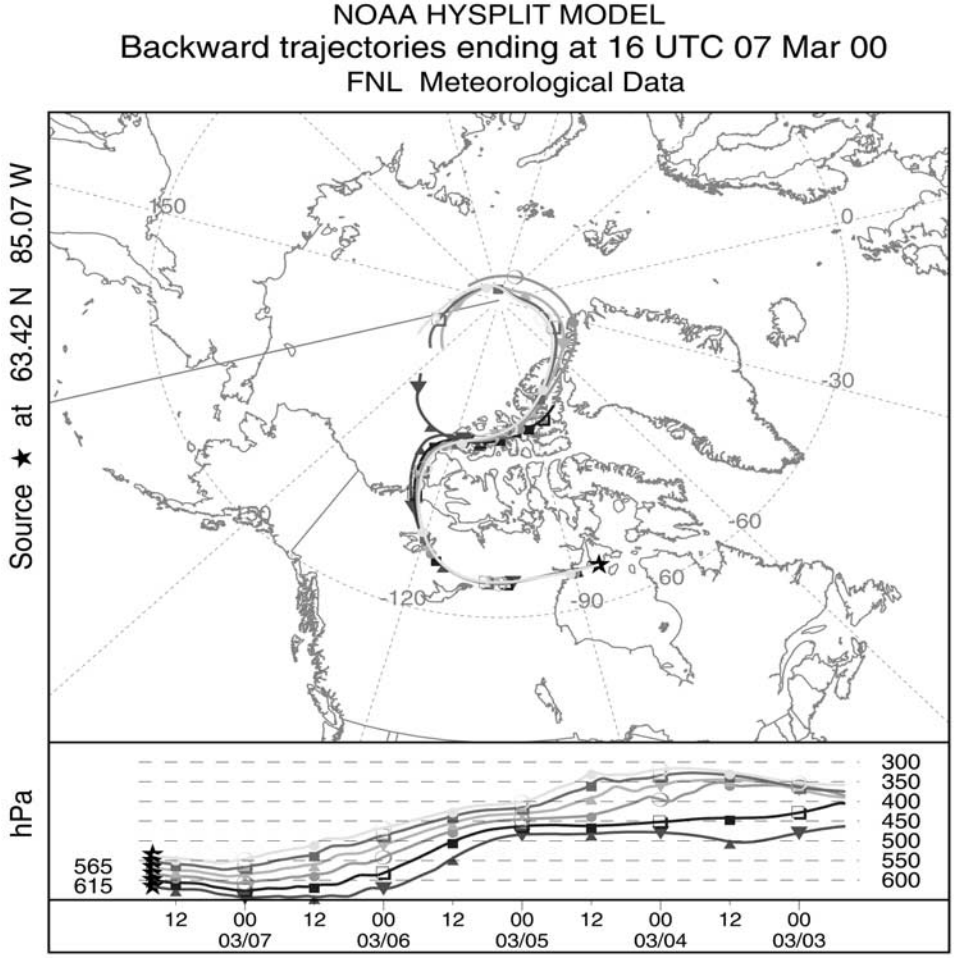

Figure 4. Five-day multiple backward trajectories calculated using NOAA Air Resources Laboratory HYSPLIT transport model PC version, from the time of observation on 7 March 2000.

Figure 5 shows a schematic, from left to right, of the air parcel track, its likely contact with the clouds, particle nucleation and cloud processing during its transport toward measurement region.

[21] The initial conditions for the model simulations (Table 1) were taken as follows: (1) the initial T and RH were calculated from air parcel backward trajectory simulations; (2) the initial particle surface area (SA), H_2SO_4 concentration and particle number concentrations were assumed to be zero (at -20 hours) because of scavenging of particles in the cloud because the parcel has come into contact with the cloud at this time (Figure 5); (3) OH concentration, which controls the H_2SO_4 source strength, via oxidation of SO_2, was prescribed using a sinusoidal diurnal cycle to give a peak noontime maximum of 1×10^6 molecules cm^{-3} [*Lawrence et al.*, 2001]; (4) ion production rate was varied from 8 to 12 ion pairs cm^{-3} s^{-1}, with altitude in this region [*Rosen et al.*, 1985] and (5) initial SO_2 concentration was prescribed to be 3.7 ppbv prior to the measurement ($\sim$3.4 ppbv) because SO_2 has chemical lifetime of $\sim$1 week [*Seinfeld and Pandis*, 1998, p. 314]. Dimethyl sulfide (DMS) concentrations were below the detection limit of 1 pptv (parts per trillion volume) on 7 March 2000 suggesting that oceanic SO_2 sources were unimportant [*Simpson et al.*, 2001]. However, the exact source of high SO_2 was unknown [*Weber et al.*, 2003]. The high SO_2 concentrations were observed on this day in a unique region (63.30°–63.48°N latitude and 84.40°–85.05°W longitude), while elsewhere SO_2 levels were at or below expected background levels along the flight track. We have also performed sensitivity studies of N_{3-4nm} and N_{3-8nm} with respect to SO_2 concentration. It can be seen from Figure 6 that with the assumed absence of preexisting particle surface area at the start of simulation, prescribed SO_2 concentration and air parcel conditions (Table 1), the nucleated particles grew slowly, and reached sizes of diameter between 3–4 nm and 3–8 nm until the time of measurement.

[22] Most numerical simulations of transport in cloud systems suggest that substantial fractions of SO_2 can be transported through vigorous convective clouds [*Barth*, 1994; *Crutzen and Lawrence*, 2000; *Kreidenweis et al.*, 1997]. However, it is unlikely that vigorous convective activity transported substantial amount of SO_2 in this region during March 2000. For the sensitivity analysis, environmental parameters selected for model simulation, were similar to those mentioned in Table 1. *Brock et al.* [2004] have performed similar numerical simulations in the free

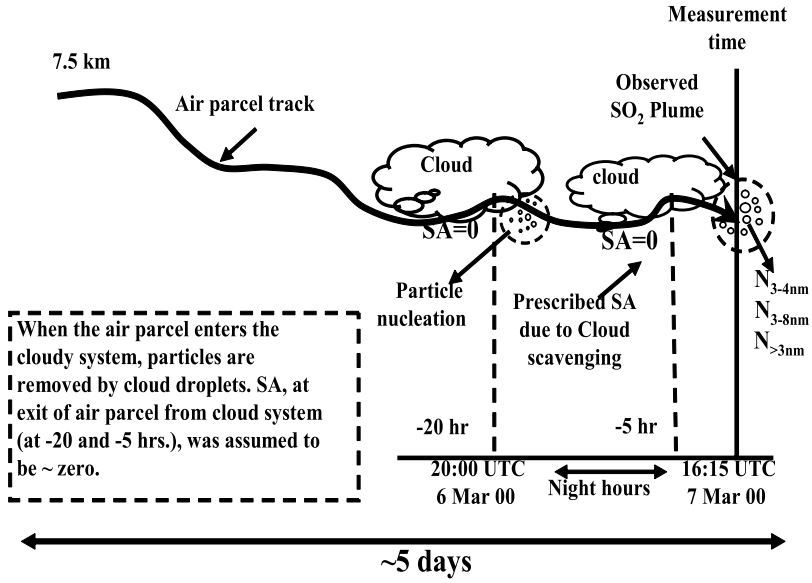

Figure 5. Schematic diagram showing, from left to right, air parcel track and its likely contact with clouds (−20 and −5 hours) during its transport toward the measurement region, cloud processing, nucleation, and condensational growth to produce observed N_{3-4nm} and N_{3-8nm} particle number on 7 March 2000.

troposphere over the eastern Pacific Ocean and the western coast of North America to interpret observed particle nucleation events.

[23] The results of the numerical simulation (Table 1) closely match the observed N_{3-4nm} and N_{3-8nm} at the end of the 20-hour run. Figure 7 shows that lowering of preexisting particle surface area indeed facilitated particle nucleation in this region for ion production rates 10–20 ion pairs cm^{-3} s^{-1}. Since the temperature did not suddenly dropped nor RH increased, it is plausible that the sudden lowering of preexisting particle surface areas may have triggered nucleation ~1 day prior to the time of measurement and then particles subsequently grew to measurable sizes until the time of observation.

[24] A unique region of high N_{3-4nm} and N_{3-8nm} was detected during this flight provided an opportunity to answer the question raised by *Weber et al.* [2003] whether the observed particles were produced in situ or transported from lower latitudes. The environmental conditions, where nucleation has been observed during this flight, were used to correlate model-predicted and observed N_{3-4nm} and N_{3-8nm}. Similar backward trajectory analysis followed by model simulations has been performed for each individual observed environmental condition. The model-predicted and in situ measured ultrafine particle number concentrations were correlated with a correlation coefficient (R) of 0.93 (Figure 8) and uncertainties in the linear curve fit coefficients within 95% confidence intervals. The model simulations suggest that ion-assisted nucleation is a plausible mechanism for new particle formation on 7 March 2000; however, other mechanisms have not been evaluated and cannot be completely ruled out.

[25] Similar analyses were also performed for the ambient measurements where no or few N_{3-4nm} and N_{3-8nm} were observed. From Figure 3c, it can be seen that air parcel is likely to come into contact with the clouds at −10 hours, during its transport toward no nucleation region. The initial condition for model simulation was prescribed in a similar way as discussed above except for SO_2. The initial SO_2 concentration in this case was assumed to be 0.1 ppbv prior to the time of measurement (~0.08 ppbv). The model did

Table 1. Environmental Parameters Used in Model Simulation and Comparison With In Situ Measured N_{3-4nm} and N_{3-8nm} Particle Number Concentrations at 1615 UTC on 7 March 2000

						Model Simulation		Measurement	
Time, hours	*T*, K	RH, %	*Q*, cm^{-3} s^{-1}	SO_2, ppbv	SA, μm^2 cm^{-3}	3–4 nm, particles cm^{-3}	3–8 nm, particles cm^{-3}	3–4 nm, particles cm^{-3}	3–8 nm, particles cm^{-3}
−20	242	50	8	3.7[a]	0.0	0.0	0.0	NM[b]	NM
−5	241	50	10	3.6	0 {134}[c]	0 {1271}[c]	0 {4238}[c]	NM	NM
−3	242	25	12	3.5	0.28	74	104	NM	NM
0	240	15	12	3.4	2.82	170	204	65 ± 10	289 ± 40

[a]OH was prescribed using a sinusoidal diurnal cycle, and initial SO_2 was prescribed to be 3.7 ppbv prior to that observed at time of measurement (~3.4 ppbv).

[b]NM, no measurements.

[c]Particle surface area and particle number were set to be zero, because of cloud processing, since air parcel is likely to come into contact with the clouds at −5 hours. Simulated particle surface area and particle number at −5 hours are given in braces.

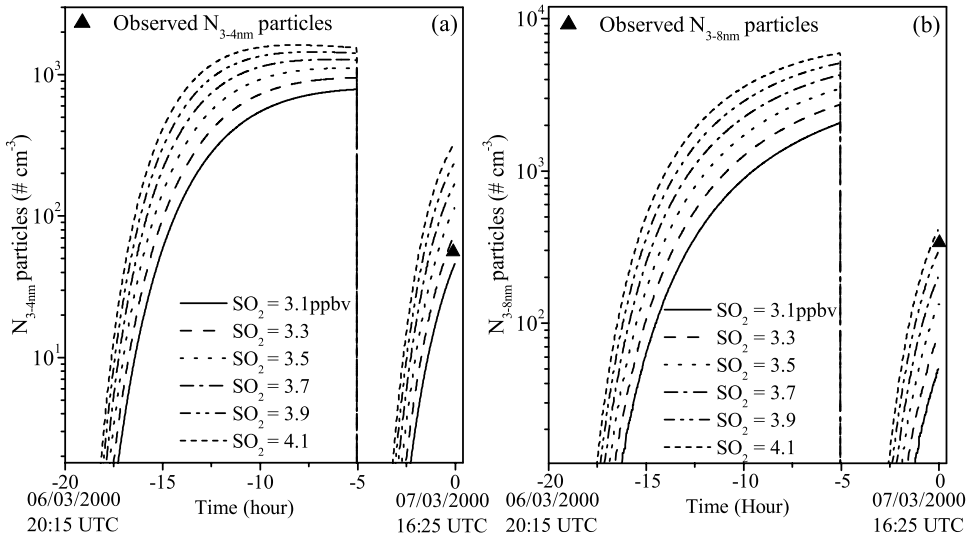

Figure 6. (a) N_{3-4nm} and (b) N_{3-8nm} particle number concentrations as a function of age of parcel (time in hours) for different SO_2 concentrations. Model simulations were performed for environmental conditions as given in Table 1 for SO_2 = 3.1, 3.3, 3.5, 3.7, 3.9, and 4.1 ppbv. In situ measured N_{3-4nm} and N_{3-8nm} particle number concentrations on 7 March 2000 are shown by bold triangle in Figures 6a and 6b, respectively.

not predict new particle formation in this region consistent with the observations (Table 2).

6. Summary and Conclusions

[26] In this paper we investigated the ion-induced particle nucleation mechanism and its controlling factors leading to new particle formation in the middle to upper troposphere. In particular we chose an atmospheric nucleation event that provided an opportunity to answer questions posed by *Weber et al.* [2003]. The appearance of high concentrations of ultrafine particles signifies recent new particle formation in this region. Previous measurements of cloud condensation nuclei near marine clouds have suggested that the enhanced RH is a key factor for the formation of new particles near clouds, as the nucleation rate is sensitive to RH. However, an interesting feature of this event is that RH

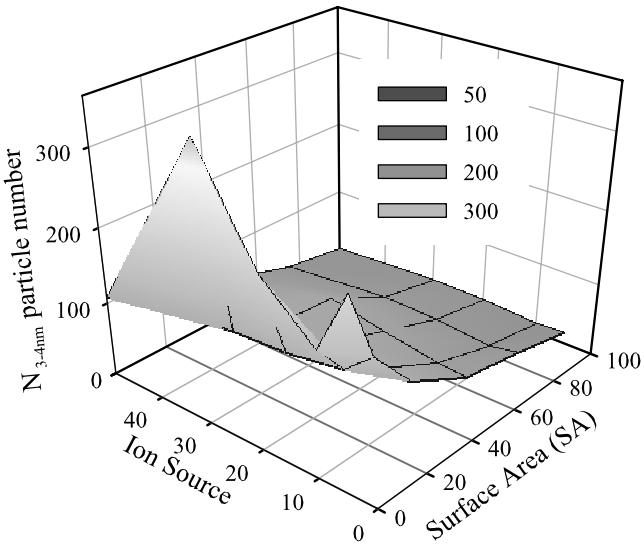

Figure 7. Model-calculated N_{3-4nm} particle number concentration at the end of simulation as a function of preexisting particle surface area and ion production rates. Model simulations were performed for in situ measured and air parcel parameters as given in Table 1 for SA = 0–100 μm^2 cm^{-3} and Q = 2–30 ion pairs cm^{-3} s^{-1}.

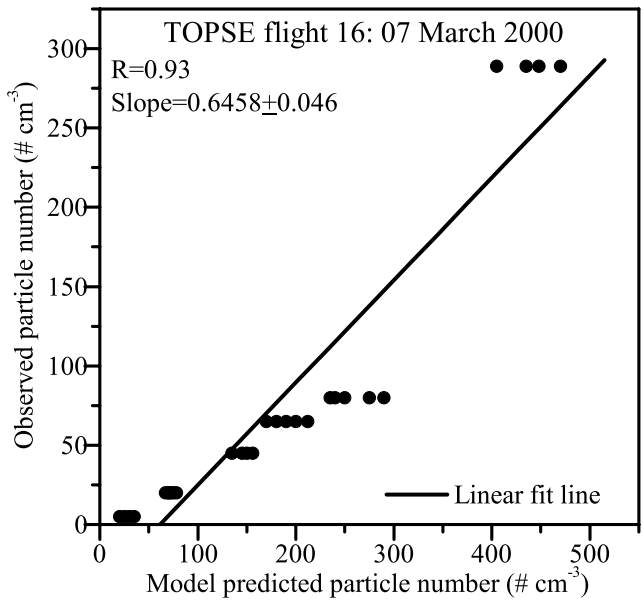

Figure 8. Comparison between in situ measured and model-predicted N_{3-4nm} and N_{3-8nm} particle number concentrations for measurements made on 7 March 2000. Multiple points at constant values of y represent model sensitivity runs over the observed range of environmental variation of T, RH, and SO_2 and for Q = 8–15 ion pairs cm^{-3} s^{-1}.

Table 2. Environmental Parameters Used in Model Simulation and Comparison With In Situ Measured N_{3-4nm} and N_{3-8nm} Particle Number Concentrations at 1535 UTC on 7 March 2000

					Model Simulation		Measurement	
Time, hours	T, K	RH, %	Q, cm^{-3} s^{-1}	SO_2, ppbv	3–4 nm, particles cm^{-3}	3–8 nm, particles cm^{-3}	3–4 nm, particles cm^{-3}	3–8 nm, particles cm^{-3}
−20	223.4	50	15	0.1[a]	0.0	0.0	NM[b]	NM
−10	235.5	50	12	0.1	0.0	0.0	NM	NM
0	228.7	15	10	0.08	0.0	0.0	0.11	0.67

[a]OH was prescribed using a sinusoidal diurnal cycle, and initial SO_2 was prescribed to be 0.1 ppbv prior to that observed at time of measurement (∼0.08 ppbv).
[b]NM, no measurements.

was found to be low (<15%) in the region of high ultrafine particles observed in TOPSE. Therefore present model simulations investigated the role played by other environmental factors, which triggered particle nucleation in the middle to upper troposphere prior to the time of measurement.

[27] The model simulated N_{3-4nm} and N_{3-8nm} were found to be in reasonable agreement with that in situ measurements on 7 March 20000 during the TOPSE experiment. Since air parcel backward trajectory simulations indicate that the air parcel was circling the pole prior to measurement, we believe that observed particles of diameter greater than 3 nm are not transported from lower latitudes; rather they were produced in situ. Our analysis also indicates that particle nucleation occurred prior to the time of measurement and subsequently particles grew over a period of −20 hours to detectable sizes at the time of observation. Low particle surface area and high SO_2 were the key factors that lead to particle nucleation in this region. Because N_{3-4nm} and N_{3-8nm} measured in the high-latitude middle to upper troposphere are consistent with the model prediction, we believe that IIN is an efficient mechanism for explaining new particle formation in the high-latitude middle to upper troposphere.

[28] **Acknowledgments.** This work is supported through a grant from the RESPOND Programme of the Indian Space Research Organisation. The authors are grateful to the Research Aviation Facility (RAF) of the National Center for Atmospheric Research (NCAR) for providing data for this study. We are thankful to Satellite Data Service, SSEC, University of Wisconsin, for providing GOES 10 Imager data sets. The authors are grateful to Ned Lovejoy and Antony Schreiner for useful discussions and suggestions. The authors are also grateful to the reviewers for their constructive suggestions.

References

Atlas, E. L., B. A. Ridley, and C. Cantrell (2003), The Tropospheric Ozone Production about the Spring Equinox (TOPSE) Experiment: Introduction, *J. Geophys. Res.*, *108*(D4), 8353, doi:10.1029/2002JD003172.

Barth, M. C. (1994), Numerical modeling of sulfur and nitrogen chemistry in a narrow cold-frontal rain band: The impact of meteorological and chemical parameters, *J. Appl. Meteorol.*, *33*, 855–868.

Brock, C. A., P. Hamill, H. H. Jonsson, J. C. Wilson, and K. R. Chan (1995), New particle formation in the upper tropical troposphere: A source for the stratospheric aerosol, *Science*, *270*, 1650–1653.

Brock, C. A., et al. (2004), Particle characteristics following cloud-modified transport from Asia to North America, *J. Geophys. Res.*, *109*, D23S26, doi:10.1029/2003JD004198.

Clarke, A. D., J. L. Varner, F. Eisele, R. L. Mauldin, D. Tanner, and M. Litchy (1998), Particle production in the remote marine atmosphere: Cloud outflow and subsidence during ACE 1, *J. Geophys. Res.*, *103*, 16,397–16,409.

Clarke, A. D., F. Eisele, V. N. Kapustin, K. Moore, D. Tanner, L. Mauldin, M. Litchy, B. Lienert, M. A. Carroll, and G. Albercrook (1999), Nucleation in the equatorial free troposphere: Favorable environment during PEM-Tropics, *J. Geophys. Res.*, *104*, 5735–5744.

Coffman, D. J., and D. A. Hegg (1995), A preliminary study of the effect of ammonia on particle nucleation in the marine boundary layer, *J. Geophys. Res.*, *100*, 7147–7160.

Crutzen, P. J., and M. G. Lawrence (2000), The impact of precipitation scavenging on the transport of trace gases: A 3-dimensional model sensitivity study, *J. Atmos. Chem.*, *37*, 81–112.

DeMore, W. B., S. P. Sander, D. M. Golden, R. F. Hampson, M. J. Kurylo, C. J. Howard, A. R. Ravishankara, C. E. Kolb, and M. J. Molina (1997), Chemical kinetics and photochemical data for use in stratospheric modeling: Evaluation number 12, *JPL Publ.*, *97-4*, 266 pp.

De Reus, M., J. Ström, P. Hoor, J. Lelieveld, and C. Schiller (1999), Particle production in the lowermost stratosphere by convective lifting of the tropopause, *J. Geophys. Res.*, *104*, 23,935–23,940.

De Reus, M., R. Krejci, J. Williams, H. Fischer, R. Scheele, and J. Strom (2001), Vertical and horizontal distribution of the aerosol number concentration and size distribution over the northern Indian Ocean, *J. Geophys. Res.*, *106*, 28,629–28,641.

Hegg, D. A., L. F. Radke, and P. V. Hobbs (1991), Measurements of Aitken nuclei and cloud condensation nuclei in the marine atmosphere and their relation to the DMS-cloud climate hypothesis, *J. Geophys. Res.*, *96*, 18,727–18,733.

Hermann, M., J. Heinzenberg, A. Wiedensohler, A. Zahn, G. Heinrich, and C. A. M. Brenninkmeijer (2003), Meridional distributions of aerosol particle number concentrations in the upper troposphere and lower stratosphere obtained by Civil Aircraft for Regular Investigation of the Atmosphere Based on an Instrument Container (CARIBIC) flights, *J. Geophys. Res.*, *108*(D3), 4114, doi:10.1029/2001JD001077.

Jacobson, M. Z. (1997), Numerical techniques to solve condensational and dissolutional growth equations when growth is coupled to reversible reactions, *Aerosol Sci. Technol.*, *27*, 491–498.

Jacobson, M. Z. (1999), *Fundamental of Atmospheric Modelling*, Cambridge Univ. Press, New York.

Jacobson, M. Z. (2002), Analysis of aerosol interactions with numerical techniques for solving coagulation, nucleation, condensation, dissolution, and reversible chemistry among multiple size distributions, *J. Geophys. Res.*, *107*(D19), 4366, doi:10.1029/2001JD002044.

Jacobson, M. Z., and R. P. Turco (1995), Simulating condensational growth, evaporation, and coagulation of aerosols using moving and stationary size grid, *Aerosol Sci. Technol.*, *22*, 73–92.

Kreidenweis, S. M., Y. Zhang, and G. R. Taylor (1997), The effects of clouds on aerosol and chemical species production and distribution: 2. Chemistry model description and sensitivity analysis, *J. Geophys. Res.*, *102*, 23,867–23,882.

Kulmala, M. (2003), How particles nucleate and grow, *Science*, *302*, 1000–1001.

Kulmala, M., L. Pirijola, and J. M. Makela (2000), Stable sulfate clusters as a source of new atmospheric particles, *Nature*, *404*, 66–69.

Kulmala, M., H. Vehkamäki, T. Petajaa, M. Dal Masoa, A. Lauria, V. M. Kerminenb, W. Birmilic, and P. H. McMurry (2004), Formation and growth rates of ultrafine atmospheric particles: A review of observations, *J. Aerosol Sci.*, *35*, 143–176.

Laakso, L., J. M. Makela, L. Pirjola, and M. Kulmala (2002), Model studies on ion-induced nucleation in the atmosphere, *J. Geophys. Res.*, *107*(D20), 4427, doi:10.1029/2002JD002140.

Lawrence, M. G., P. Jockel, and R. von Kuhlmann (2001), What does the global mean OH concentration tell us?, *Atmos. Chem. Phys.*, *1*, 37–49.

Lee, S. H., J. M. Reeves, J. C. Wilson, D. E. Hunton, A. A. Viggiano, T. M. Miller, J. O. Ballenthin, and L. R. Lait (2003), New particle formation by ion-induced nucleation in the upper troposphere and lower stratosphere, *Science*, *310*, 1886–1889.

Lee, S.-H., et al. (2004), New particle formation observed in the tropical/subtropical cirrus clouds, *J. Geophys. Res.*, *109*, D20209, doi:10.1029/2004JD005033.

Lovejoy, E. R., J. Curtius, and K. D. Froyd (2004), Atmospheric ion-induced nucleation of sulfuric acid and water, *J. Geophys. Res.*, *109*, D08204, doi:10.1029/2003JD004460.

Marti, J. J., R. J. Weber, P. H. McMurry, F. Eisele, D. Tanner, and A. Jefferson (1997), New particle formation at a remote continental site: Assessing the contributions of SO_2 and organic precursors, *J. Geophys. Res.*, *102*, 6331–6340.

Modgil, M. S., S. Kumar, S. N. Tripathi, and E. R. Lovejoy (2005), A parameterization of ion-induced nucleation of sulphuric acid and water for atmospheric conditions, *J. Geophys. Res.*, *110*, D19205, doi:10.1029/2004JD005475.

Nyeki, S., M. Kalberer, M. Lugauer, E. Weingartner, A. Petzold, F. Schröder, I. Colbeck, and U. Baltensperger (1999), Condensation nuclei (CN) and ultrafine CN in the free troposphere to 12 km: A case study over the Jungfraujoch high-alpine research station, *Geophys. Res. Lett.*, *26*, 2195–2198.

O'Dowd, C. D., J. L. Jimenez, R. Bahraini, R. C. Flagan, J. H. Seinfeld, K. Mammary, L. Pirjola, K. Kulmala, S. G. Jennings, and T. Hoffmann (2002), Marine aerosol formation from bioorganic iodine emissions, *Nature*, *417*, 632–636.

Perry, K. D., and P. V. Hobbs (1994), Further evidence for particle nucleation in clean air adjacent to marine cumulus clouds, *J. Geophys. Res.*, *99*, 22,803–22,818.

Rosen, J. M., D. J. Hoffmann, and W. Gringel (1985), Measurements of ion mobility to 30 km, *J. Geophys. Res.*, *90*, 5876–5884.

Schreiner, A. J., T. J. Schmit, and W. P. Menzel (2001), Observations and trends of clouds based on GOES sounder data, *J. Geophys. Res.*, *106*, 20,349–20,363.

Schröder, F., and J. Ström (1997), Aircraft measurements of sub micrometer aerosol particles (>7 nm) in the midlatitude free troposphere and tropopause region, *Atmos. Res.*, *44*, 333–356.

Seinfeld, J. H., and S. N. Pandis (1998), *Atmospheric Chemistry and Physics*, John Wiley, Hoboken, N. J.

Simpson, I. J., J. J. Colman, A. L. Swanson, A. R. Bandy, D. C. Thornton, D. R. Blake, and F. S. Rowland (2001), Aircraft measurements of dimethyl sulfide (DMS) using a whole air sampling technique, *J. Atmos. Chem.*, *39*, 191–213.

Tripathi, S. N., X. P. Vancassel, R. G. Grainger, and H. L. Rogers (2004), A fast Stratospheric Aerosol Microphysical Model (SAMM): H_2SO_4-H_2O aerosol development and validation, *AOPP Memo. 2004.1*, Dep. of Phys., Univ. of Oxford, Oxford, UK.

Uhrner, U., W. Birmili, F. Stratmann, M. Wilck, I. J. Ackermann, and H. Berresheim (2003), Particle formation at a continental background site: Comparison of model results with observations, *Atmos. Chem. Phys.*, *3*, 347–359.

Vehkamäki, H., M. Kulmala, I. Napari, K. E. J. Lehtinen, C. Timmreck, M. Noppel, and A. Laaksonen (2002), An improved parameterization for sulfuric acid–water nucleation rates for tropospheric and stratospheric conditions, *J. Geophys. Res.*, *107*(D22), 4622, doi:10.1029/2002JD002184.

Wang, Y., S. C. Liu, B. E. Anderson, Y. Kondo, G. L. Gregory, G. W. Sachse, S. A. Vay, D. R. Blake, H. B. Singh, and A. M. Thompson (2000), Evidence of convection as a major source of condensation nuclei in the northern midlatitude upper troposphere, *Geophys. Res. Lett.*, *27*, 369–372.

Weber, R. J., P. H. McMurry, L. Mauldin, D. Tanner, F. Eisele, A. Clarke, and V. N. Kapustin (1999), New particle production in the remote troposphere: A comparison of observations at various sites, *Geophys. Res. Lett.*, *26*, 307–310.

Weber, R. J., G. Chen, D. D. Davis, R. L. Mauldin, D. J. Tanner, F. L. Eisele, A. D. Clarke, D. C. Thornton, and A. R. Bandy (2001), Measurements of enhanced H_2SO_4 and 3–4 nm particles near a frontal cloud during ACE 1, *J. Geophys. Res.*, *106*, 24,107–24,117.

Weber, R. J., et al. (2003), Investigations into free tropospheric new particle formation in the central Canadian arctic during the winter/spring transition as part of TOPSE, *J. Geophys. Res.*, *108*(D4), 8357, doi:10.1029/2002JD002239.

Yu, F., and R. P. Turco (2001), From molecular clusters to nanoparticles: Role of ambient ionization in tropospheric aerosol formation, *J. Geophys. Res.*, *106*, 4797–4814.

V. Kanawade and S. N. Tripathi, Department of Civil Engineering, Indian Institute of Technology, Kanpur 208016, India. (snt@iitk.ac.in)